

# THE EFFECTS OF ARBITRARY INJECTION ANGLE AND FLOW CONDITIONS ON VENTURI-JET MIXER

by

**S.SUNDARARAJ, V.SELLADURAI**

*This paper describes the effect of jet injection angle, cross flow Reynolds number and velocity ratio on entrainment and mixing of jet with incompressible cross flow in venturi-jet mixer. Five different jet injection angles 45°, 60°, 90°, 125°, 135° are tested to evaluate the entrainment of jet and mixing performances of the mixer. Tracer concentration along the downstream of the jet injection, cross flow velocity, jet velocity and pressure drop across the mixer are determined experimentally to characterise the mixing performance of the mixer. The experiments show that the performance of a venturi-jet-mixer substantially improves at high injection angle and can be augmented still by increasing velocity ratio. The jet deflects much and penetrates less in the cross flow as the cross flow Reynolds number is increased. The effect could contribute substantially to the better mixing index with moderate pressure drop. Normalised jet profile, concentration decay, jet velocity profile are computed from equations of conservation of mass, momentum and concentration written in natural co-ordinate systems. The comparison between the experimental and numerical results confirms the accuracy of the simulations. Correlations for jet trajectory and entrainment ratio of the mixer are obtained by multivariate-linear regression analysis using power law.*

*Key words: jet injection, static mixer, incompressible flow, proportional mixing, concentration decay*

## 1. Introduction

The intensive use of static mixers in the industrial processes is dated around the 1970s. The difference between the mixing in a normal pipeline and in a pipeline equipped with a static mixer is apparent. In turbulent flow, static mixers create a higher degree of turbulence as compared to a normal pipe, thereby resulting in a higher degree of mixing dispersion and/or mass transfer [1]. An empty tube working in turbulent flow regime is the simplest static mixer, however it is necessary a length nearly equal to 100 pipe diameters for complete mixing. On the contrary, if static mixers are used, the complete mixing can be obtained with a length nearly equal to 4-6 diameters [2]. Cross flow mixing is used in many applications where the objective is to rapidly obtain a homogeneous mixture of the injectate and mainstream. The mixing process is affected by a number of parameters and optimization of the process in a confined duct has been the topic of several recent investigations [3-5]. The challenge to further increase mixing rates without a corresponding increase in pressure drop is being met by efforts to exploit 'passive' techniques to enhance mixing. The use of 'passive' methods to control mixing has been widely studied in axi-symmetric free jets [6, 7].

In the recent years, venturi-jet mixer systems have received great attention by many researchers and they have been widely applied to the fluid mixing area [8-10]. Considerable advantages are conferred by the venturi-jet mixer, such as shorter mixing length, parallel operations and passive mixing. Venturi-jet mixers are generally thought to be most effective means for proportionally mixing the jets with cross flow. Controlling the fluid motions and mixing for applications in engineering and environmental aspects, the study of jet exhausting in cross flow of venturi-jet mixer is an important aspect. The mixing of fluids at required proportions are possible by

the suction effect created in the venturi-jet mixer. The mixing layer grows in the direction of jet flow, entraining and mixing the cross flow into the jet. Venturi-jet mixers can be used in place of agitators in practically all the cases where the liquids to be mixed can be pumped. Recent studies of mixing in venturi-jet mixers have shown that the mixing unit can be used for mixing two fluid streams like water and soil conditioning fluid, desalination of seawater and diluting the concentrates and mixing flavourings [11-13]. They also showed that mixing characteristics were determined with regard to mixing ratio and improved by free stream turbulence and mainstream swirl. The evident also suggests that no manipulation was required and the intimate mixing could be obtained in the course of distribution.

Margason [14] provided an extensive review of past work before 1993 on jet in cross flow. In many of the studies, the main interests are the trajectories prediction, the formation, evolution and interaction of the counter-rotating vortex- pair (CVP) and their respective applications. Both experimental and computational efforts were conducted to investigate the details of different flow structures of JICF. Maruyama *et al.* [15, 16] studied the jet injection of fluid into the pipeline over several pipe diameters from the injection point, and proposed the standard deviation as an indication of mixing quality. The dilution characteristics and the plume trajectory of the tee diffusers have been studied by several investigators in order to provide basic information for the siting and design of the diffuser [17, 18]. A heated and unheated lateral jets discharging into a confined swirling cross flow was numerically investigated by Chao and Ho [19]. They studied variations of parameters like jet temperature, jet-to-cross flow velocity ratio, jet number and swirl length. The results show that the jet decaying process is almost independent of the temperature difference between the heated jet and the cross flow. Sarkar and Bose [20], predicted characteristics of a two-dimensional turbulent plane jet in a cross flow where a cold jet stream is discharged into a strong cross stream ( $R \leq 1.0$ ). They computed flow field and surface temperature distributions along with the turbulence quantities to illustrate the flow physics involved.

Su and Mungal [21] conducted experiments to analyse the structure and scaling of the velocity and scalar fields using PIV and PLIF measurement techniques. The measurements provided a comprehensive view of the velocity and conserved scalar fields in the developing region of the flow. All measurements are made at a single jet-to-cross flow velocity ratio of 5.7. Amighi *et al.* [22] presented experimental results on the penetration of a water jet in a cross flow under atmospheric and elevated pressures and temperatures. Images of the jet at various test conditions were obtained, using pulsed laser sheet illumination technique. Stephen [23] studied the characteristics of siphon-jet flows for several geometric configurations and flow speeds. A general method for optimising the design of liquid / liquid jet pumps was suggested by Vyas and Kar [24] in which component dimensions (suction nozzle, driving nozzle, mixing tube and diffuser) were expressed as dimensionless ratios. They described the entrainment of the suction fluid by viscous friction and acceleration of the resulting mixture by momentum transfer with the driving fluid in the mixing tube (throat); complete mixing was assumed by the end of the throat, as is the case with other researchers [25, 26].

Previous research on passive mixing by venturi-jet mixer has concentrated on typically one of the geometric factors, and an overall view of geometric configuration and their effect on mixing is not clear. The present work on the study of mixing in venturi-jet mixer considers the effect of jet injection

angle, jet-cross flow momentum ratio and Reynolds number on jet trajectory and mixing efficiency of incompressible cross flow with jet. Enhancement of the mixing rate between jet and cross flow can lead to significant improvements in many performance aspects. The paper reports on experimental concentration in downstream locations and overall pressure drop for the incompressible fluids mixing in the mixer. This work builds upon a previously reported study by Sundararaj & Selladurai [27], in which the jet injection of incompressible flow in venturi-jet mixer was investigated. The flow field of a vertical jet in cross flow is observed to be primarily influenced by the square root of fluid momentum ratio

$$R = \left[ \frac{\rho_j u^2}{\rho_{cf} v^2} \right]^{1/2} \quad (1)$$

written here as an effective velocity ratio,  $R = u/v$  for incompressible flows, where  $u$  is the jet velocity,  $v$  is the cross flow velocity,  $\rho_j$  is the density of jet,  $\rho_{cf}$  is the density of cross flow. The local scalar concentration maxima, jet velocity profile and jet width in downstream are obtained from the numerical simulation. The experimental results are used to validate the numerical results for the mixing characteristics of venturi-jet mixer using local scalar concentration maxima. In addition, jet trajectories normalised with  $d$ ,  $Rd$  and  $R^2d$  as proposed by Li *et al.* [28] are computed for arbitrary injection angles and compared with the results of Yuan & Street [29].

## 2. Materials and methods

### 2.1 Cross flow and jet fluids

For the experiments, a tracer solution of potassium-di-chromate with concentration of 0.3% is prepared by dissolving dry potassium dichromate in distilled water at ambient temperature. Water with no tracer concentration is used as cross flow in the mixer. The tracer fluid had the same viscosity as the main fluid. The other properties of tracer liquid determined and are equal to the properties of water with a difference of  $\pm 2\%$ .

### 2.2 Experimental setup and operation

Experiments are conducted in a transparent Plexiglas rod, machined inside to the shape of venturi and jet placed in throat at an arbitrary angle to evaluate the mixing. The diameter of jet is 1mm and that of throat is 10mm. A contraction ratio of 0.3025 corresponding to exit-plane area of 314.16mm<sup>2</sup> is adopted for venturi design. The contraction provides smooth uniform flow in the throat section of mixer. An optimised converging cone angle of 17° and diverging cone angle of 8.5° for maximum entrainment of suction fluid proposed by Baylar *et al.* [30] is used in the present study. The distance between the jet exit and the tracer fluid in container is 10cm for undisturbed flow of tracer. All the experiments are performed at ambient temperature. Twenty five experiments are conducted in which the jet injection angle  $\theta$  varied 45° - 135° and the cross flow Reynolds number  $Re_{cf}$  varied 58002-104403.

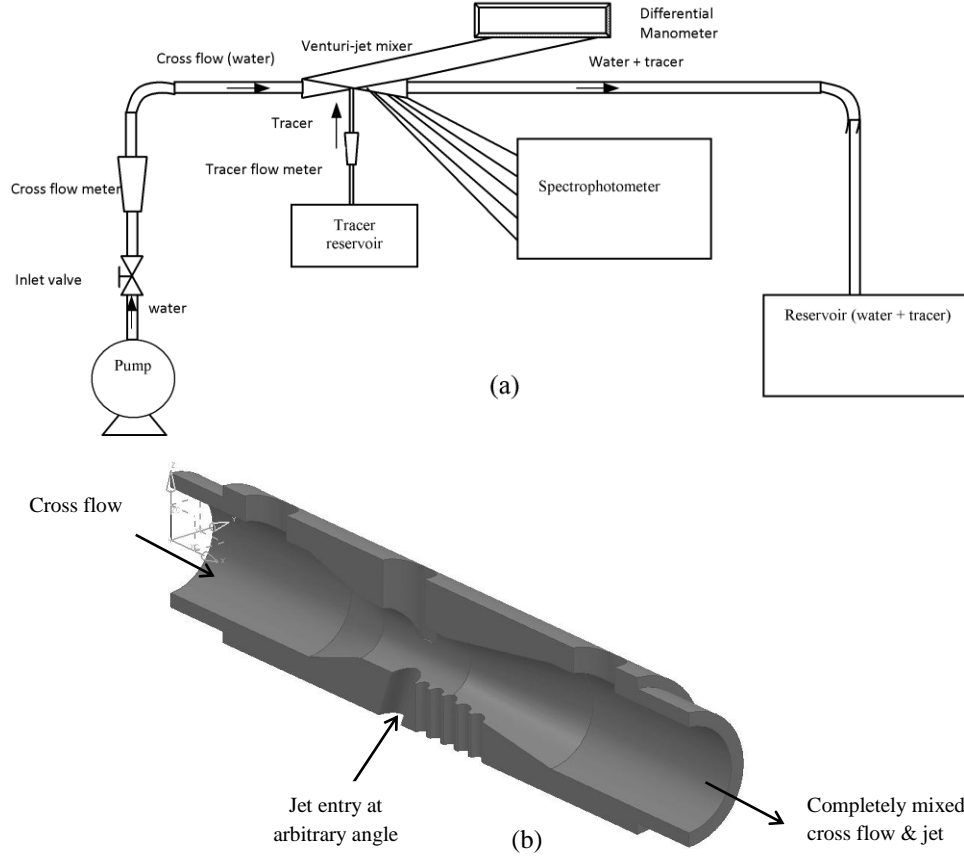


**Fig. 1** (a) Schematic representation of experimental apparatus, (b) Defining sketch of venturi-jet mixer

A digital spectrophotometer is used throughout all the experiments to measure the local scalar concentration  $c$ , operates between wavelength of 360nm and 960nm. The spectral resolution and wavelength are set as 1 and 460nm. The accuracy and repeatability of the instrument is  $\pm 3$ nm. In the present investigation, the concentration of tracer is measured along the normalised stream-wise direction for  $5d$ ,  $10d$ ,  $15d$ ,  $20d$ ,  $25d$  and  $30d$  where  $d$  is the jet diameter. The pressure drop across the venturi-jet mixer is determined with differential manometer. The flow of cross flow and jet are measured with flow metering device. The test facility shown in Fig. 1 is used to investigate the effects of the following ranges of jet injection angle and operating conditions:

- (i) Initial jet injection angles of  $45^\circ - 135^\circ$ .
- (ii) Cross flow velocities of 4.3844 – 7.8917m/s.
- (iii) Initial jet velocities 2.9958 – 5.8272 m/s.
- (iv) Velocity ratios 0.6833 – 0.8117.
- (v) Motive cross flow pressures 109.32 – 140.82 kPa (abs).
- (vi) Throat vacuum pressures 92.65 – 77.35 kPa (abs).

The flow conditions are characterised by means of three global non-dimensional parameters:

$$Re_{cf} = \frac{vD}{\gamma}; Re_j = \frac{ud}{\gamma}; R = \frac{u}{v}$$

where  $Re_{cf}$  is the cross flow Reynolds number,  $Re_j$  is the jet Reynolds number,  $\gamma$  is the kinematic viscosity of the fluid and  $D$  is the throat diameter.

### 3. Numerical formulation

A jet in cross flow, or a transverse jet, in a flow field where a jet of fluid enters and interacts with a cross flowing fluid. The JICF is a very pleasant flow configuration with regard to mixing. It is one of the most effective ways to mix two fluids in a limited space, which is superior to other flow constellations like the mixing layer or the jet in cross flow [31]. A natural coordinate system is used to develop mathematical model for incompressible transverse jet discharge into cross flow of venturi-jet mixer due to suction effect at large Reynolds number shown in Fig. 2. Based on the work of Hoult *et al.*, the governing equations modified for the present work include the conservation of mass, tangential momentum, radial momentum and concentration [32]. Most theoretical attempts to explain the jet motion involve integral methods, and, of necessity, many simplifying assumptions, particularly with regard to entrainment [31]. Equations (1a) and (1b) expressing the co-ordinate transformation between  $(x,z)$  and  $(s,\theta)$  are given by:

$$x = \int \cos\theta ds \quad (1a)$$

$$z = \int \sin\theta ds \quad (1b)$$

The conservation equations, written in natural coordinate system in ordinary differential form, are [27]:

$$\frac{d}{ds}(\pi b^2 \rho u) = 2\pi b \rho u_e \quad (2)$$

$$(\pi b^2 \rho u^2) \frac{d\theta}{ds} = -\pi b^2 \Delta p \cos\theta - v \sin\theta \frac{d}{ds}(\pi b^2 \rho u) \quad (3)$$

$$\frac{d}{ds}(\pi b^2 \rho u^2) = -b^2 \Delta p \sin\theta + v \cos\theta \frac{d}{ds}(\pi b^2 \rho u) \quad (4)$$

$$\frac{d}{ds}(\pi b^2 c u) = 0 \quad (5)$$

where  $b$  is the jet radius,  $c$  is the tracer concentration,  $x$  is the axial distance of venturi-jet mixer,  $z$  is the radial direction co-ordinate of venturi-jet mixer,  $s$  is the axial jet arc length,  $\Delta p$  is the pressure drop and  $\theta$  is the coordinate expressing the inclination of the jet centreline to the horizon.

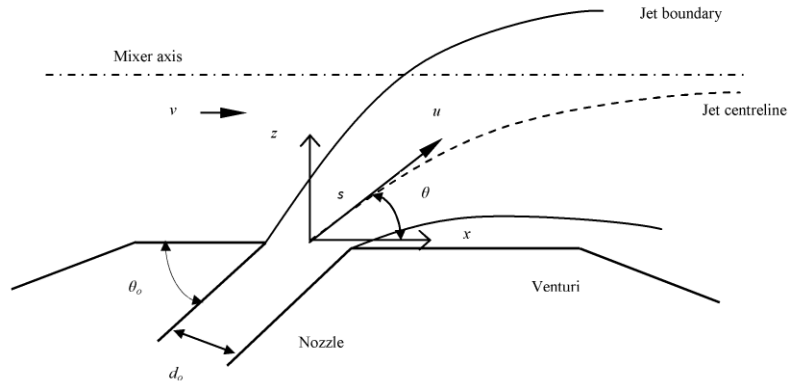


**Fig. 2** Coordinate system for jet discharge into cross flow of venturi-jet mixer

The local entrainment velocity is assumed to be

$$u_e = \alpha |u - v \cos\theta| + \beta |v \sin\theta| \quad (6)$$

where  $\alpha$  and  $\beta$  are the radial and cross flow entrainment parameter. The values of radial ( $\alpha=0.11$ ) and cross flow entrainment parameter ( $\beta=0.6$ ) suggested by Forney et al., for transverse tube flow mixers used for the current study [33]. The jet properties such as velocity and tracer concentration are assumed to have top hat profiles due to its simplicity in analysis. Fourth order Range-Kutta method is used to solve the derived conservation equations along with entrainment velocity for jet trajectory, concentration decay and velocity profile by applying the boundary conditions  $s = 0, u = u_o, c = c_o, \theta = \theta_o, b = b_o$ . The cross flow velocity  $v$  is varied 4.38-7.89 m/s and the velocity ratio  $R$  obtained is in the range 0.614-0.812. From the numerical results, jet velocity profile, concentration decay profile, the jet trajectory, jet radius growth in the parametric form  $x=x(s), z=z(s), b=b(s), u=u(s)$  and  $c=c(s)$  and mixing characteristics are obtained. The concentration decay and jet trajectory are compared with experimental results for various jet injection angle  $\theta_o$  ( $45^\circ$ - $135^\circ$ ) and cross flow Reynolds number  $Re_{cf}$  (58002-104403).

## 4. Results and discussion

### 4.1 Concentration decay and jet velocity profile

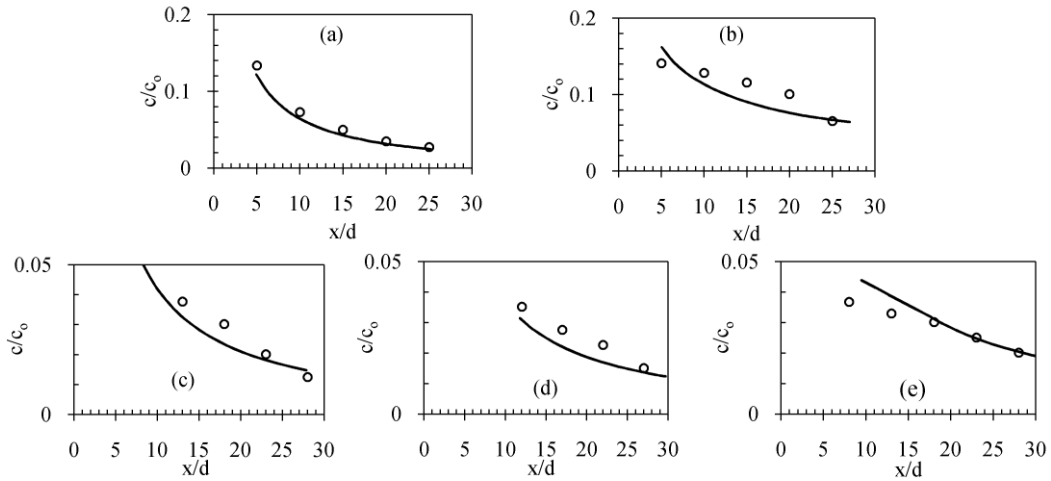


**Fig. 3** Comparison of observed and predicted centreline dilution (a)  $\theta_o - 45^\circ, Re_{cf} - 58002$ , (b)  $\theta_o - 60^\circ, Re_{cf} - 69602$ , (c)  $\theta_o - 90^\circ, Re_{cf} - 81202$ , (d)  $\theta_o - 120^\circ, Re_{cf} - 92803$ , (e)  $\theta_o - 135^\circ, Re_{cf} - 104403$ : (o experimental results, — numerical results)

The centreline decay is one of the parameters that could be used to evaluate large scale mixing [28]. Fig. 3 shows the comparison of concentration decay from numerical and experimental results for all jet injection angles and cross flow Reynolds number. The concentration of the mixture is normalised by the initial concentration of the tracer at the jet exit. The observation shows that larger injection angle  $\theta_o$  have higher decay at the same distance downstream. It is also observed that the numerical data is much closer to the experimental data. The concentration decay is rapid up to  $x=15d$  for  $\theta_o \leq 90^\circ$  and  $x=20d$  for  $\theta_o > 90^\circ$ . The reason for this is the jet expands quickly in the mixer due to turbulent entrainment and thus creates efficient macro mixing [34]. Also Fig. 3 shows the behaviour of centreline dilution. At cases when the initial jet angle is  $45^\circ$ , results of numerical simulations of centreline dilution are consistent with experimental results in both the near field and far field. However, model underestimates the data in the near and intermediate field for  $\theta_o > 45^\circ$ .

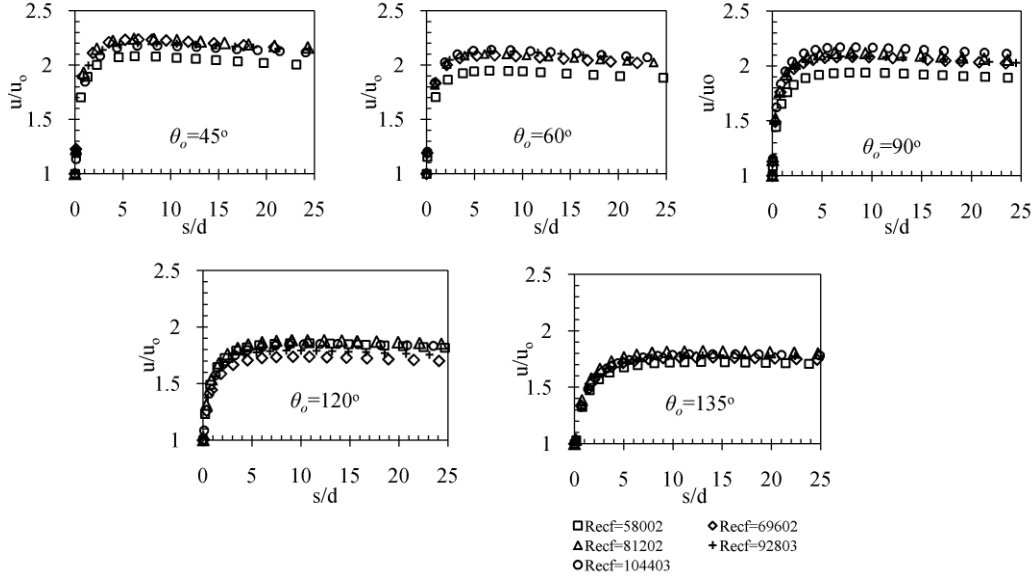


**Fig. 4** Predicted maximum jet velocity decay along trajectory for jet injection angle  $\theta_o$  :  $45^\circ$ ,  $60^\circ$ ,  $90^\circ$ ,  $120^\circ$ ,  $135^\circ$

In Fig. 4 the non-dimensional jet velocity profile plots for 5 injection angles are shown as a function of non-dimensionalised downstream distance for all the cross flow Reynolds number. The plots show that the normalised jet centreline velocity increase at rapid rate from injection point( $s=0$ ) to  $s=5d$  and uniform thereafter for all the cases of downstream distance( $s>5d$ ). Due to the mixing of the two streams with momentum ratio  $R<1$ , the local maximum jet mean velocity ( $u$ ) approaches the cross flow velocity in the downstream. Lower the cross flow Reynolds number, lower is the velocity magnitude of jets in cross flow. There is little effect on the jet velocity profile for injection angles  $45^\circ$ - $135^\circ$  with the variation of cross flow Reynolds number.

#### 4.2 Velocity ratio and Entrainment ratio

The velocity ratio,  $R$  and the entrainment ratio,  $m_j/m_{cf}$  for all the experimental cases of venturi-jet mixer for runs with different cross flow Reynolds number,  $Re_{cf}$  are shown in Fig. 5(a-c) where  $m_j$  is the mass flow of jet and  $m_{cf}$  is the mass flow of cross flow. Figure 5a indicate the lower the cross flow velocity  $v$  and Reynolds number  $Re_{cf}$ , more the jet entrains into the mixer and higher the velocity ratio  $R$  for  $45^\circ \leq \theta_o \leq 135^\circ$ . At cross flow velocity  $v=4.3844$  m/s, a higher vacuum pressure prevails in the throat which sucks more suction fluid (jet) in to the mixer for all the cases investigated. As cross flow velocity  $v$  increases, the vacuum pressure decreases at all the injection angles which results in suction effect increase. On the contrary, velocity ratio and jet entrainment rate are decreasing as the cross flow Reynolds number increase. The entrainment rate of jet is influenced by the cross-section of the inlets of venturi and jet, cross flow velocity, level of tracer liquid from centre of venturi. From Fig. 5c it is concluded that the mass entrainment with velocity ratio can be described by a linear fit.

$$\frac{m_j}{m_{cf}} = 0.008265 \left( \frac{u}{v} \right) \quad (7)$$

Equation (7) shows that the velocity ratio has an effect on mass entrainment ratio because the mass entrainment is proportional to the velocity ratio. The pre-factor and exponent in the correlation

could be functions of other parameters, such as cross flow and jet properties, the dimensions of the venturi-jet mixer and the angle of initial injection of jet.

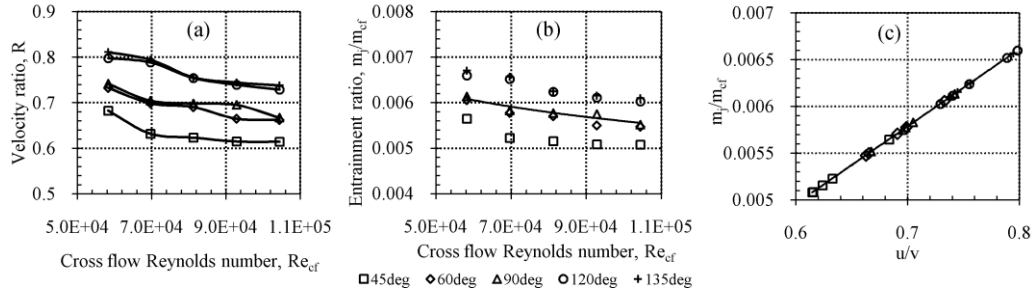


**Fig. 5** (a) Velocity ratio,  $R$  and (b) Entrainment ratio for all cases of mixer system (c) Linear fit for velocity ratio,  $u/v$  Vs entrainment ratio,  $m_j/m_{cf}$ .

#### 4.3 Jet trajectories and jet radius growth

In the present work, the local velocity maxima and local scalar concentration maxima are used for describing the jet trajectory [29, 35]. The jet trajectories for all 5 injection angles are plotted with three different normalisations:  $d$ ,  $Rd$  and  $R^2d$  as proposed by Li *et al.*[28]. Figure 6(a&b) shows simulated jet trajectory normalised with  $d$  in double logarithmic scale for jet injection angle of  $45^\circ$  and  $135^\circ$ , and compares the trajectory of Yuan and Street [29] ( $d=13.44\text{mm}$ ,  $R=2$  and  $Re_{cf}=2100$ ). It appears obvious from Fig. 3 that the jet injection angle,  $\theta_o$  and cross flow Reynolds number,  $Re_{cf}$  had a greater effect on jet penetration and deflection. Physically, an increase in jet injection angle, results in an increase in jet penetration. While the cross flow is stronger, the centre-line trajectory is more deflected and the jet penetration is reduced. Figure 6 displays a larger jet penetration for the lower cross flow Reynolds number ( $Re_{cf} = 58002$ ) and follow on the top branch, while the lower set of points relate to  $Re_{cf} = 104403$ . The numerical solutions slightly underestimate the trajectories at injection angles less than  $90^\circ$  as compared with the trajectory of Yuan and Street [29]. But at lower injection angle and cross flow Reynolds number, the jet trajectory is somewhat more in agreement with the trajectory of Yuan and Street [29].

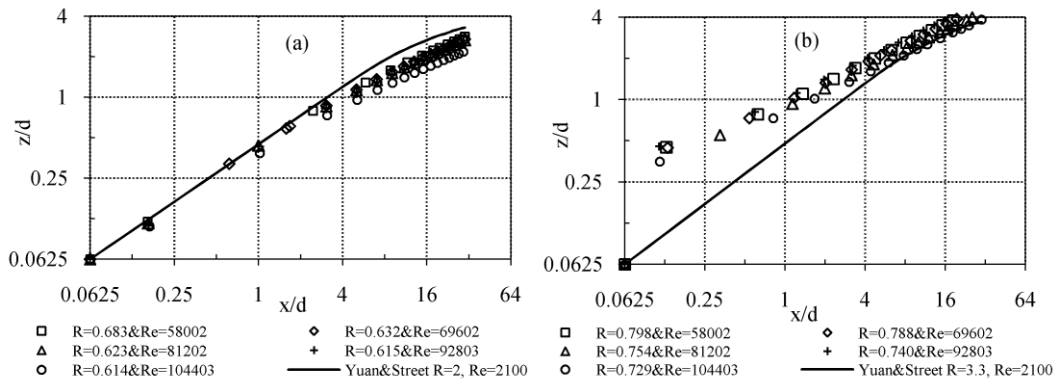


**Fig. 6** Jet trajectory normalised with  $d$  for jet injection angle,  $\theta_o$  (a)  $45^\circ$  and (b)  $135^\circ$

Figure 7(a-f) shows typical jet trajectories normalised with  $Rd$  and  $R^2d$  for injection angles  $45^\circ \leq \theta_o \leq 135^\circ$ , in double logarithmic scales for the all values of  $Re_{cf}$ . As it is drawn on double scale, the power-law relationship appears as straight line. The jet trajectory is directly dependent upon the



parameters such as jet injection angle  $\theta_o$ , momentum ratio  $R$ , cross flow Reynolds number  $Re_{cf}$ , and jet Reynolds number  $Re_j$  [22, 36].

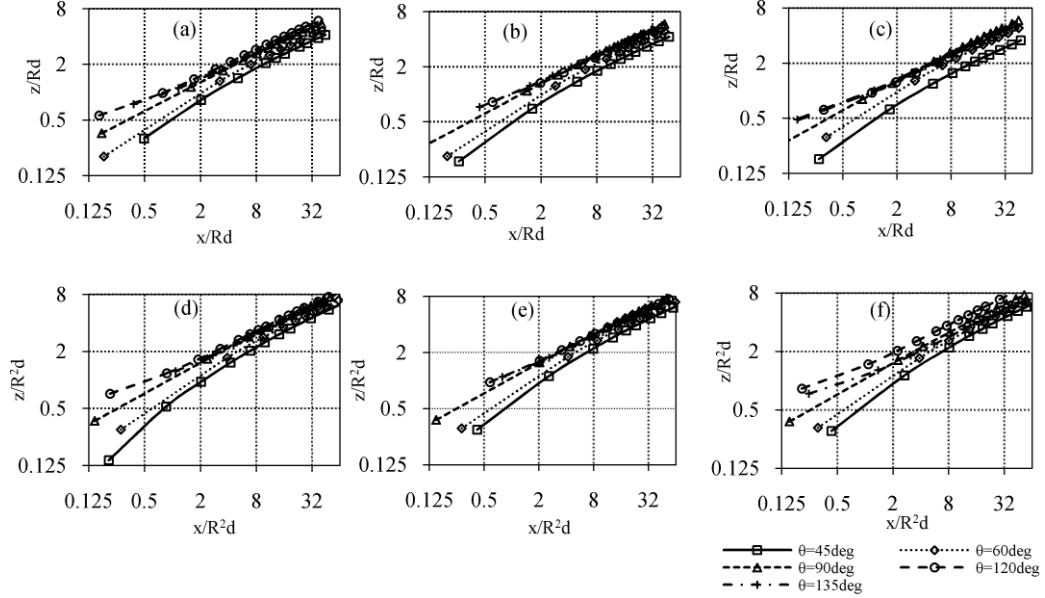


**Fig. 7** Jet trajectory normalised with  $Rd$ , (a)  $Re_{cf} = 58002$ , (b)  $Re_{cf} = 81202$ , (c)  $Re_{cf} = 104403$   
 Jet trajectory normalised with  $R^2d$ , (d)  $Re_{cf} = 69602$ , (e)  $Re_{cf} = 81202$ , (f)  $Re_{cf} = 92803$

Often this functional dependence is best characterised by multivariate power equations. For jet trajectories of all jets, an equation is obtained for jet centreline by multivariate-linear regression analysis by using power law owing to its simplicity and popularity [37]. The correlation of jet trajectory for jet in cross flow in venturi-jet mixer is obtained as given in Eq. (8):

$$\frac{z}{Rd} = \left(0.614 - 0.0047(90^\circ - \theta_o)\right) \left(\frac{x}{Rd}\right)^{0.502} R^{0.333} Re_{cf}^{0.0187} Re_j^{0.0176} \quad (8)$$

The coefficients are generated with 95% of confidence intervals. The coefficient of determination is 0.938 and the standard error is 0.37 for the jet trajectory correlation. The difference between the jet trajectory of correlation and numerical simulation is within  $\pm 10\%$  at any location. The jet upper and lower boundary trajectories are simulated using Eq. (2)-(6) with the initial conditions for cross flow speed, jet radius, axial jet velocity and the concentration of tracer.

Figure 8 displays the jet radius growth for injection angles  $45^\circ \leq \theta_o \leq 135^\circ$  and cross flow Reynolds number 58202 and 104403. The jets observed here show a faster growth in the radius along the stream wise direction for higher injection angle and consistently a slower radius growth with increase in cross flow Reynolds number. It reveals that the jet expands, penetrates and mixes with cross flow in the downstream direction. Also it is observed that much faster deflection of jet from their initial direction for higher cross flow Reynolds number  $Re_{cf}$  for a particular injection angle because of relatively small momentum ratio  $R$  and predominance of conservation of momentum in the cross flow direction.

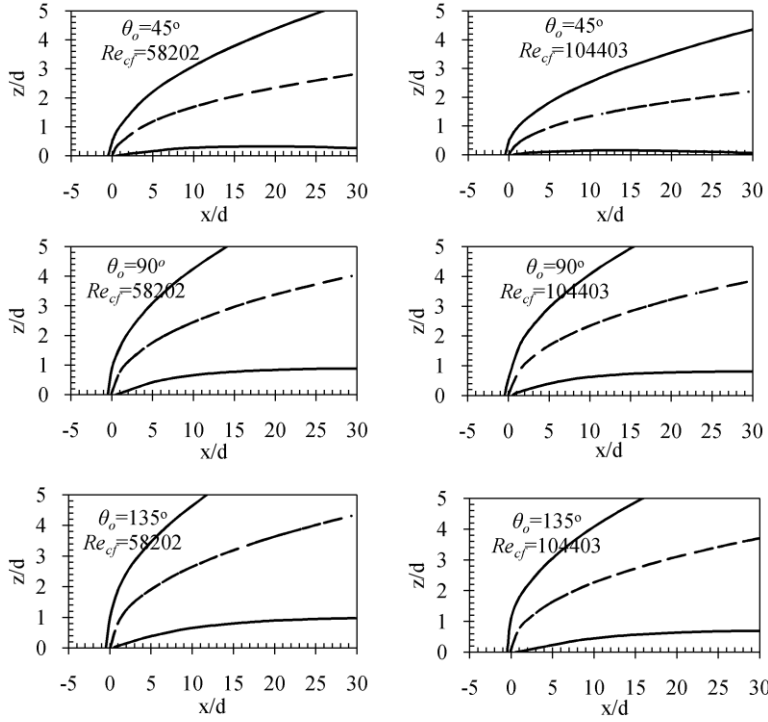


**Fig. 8** Jet radius normalised with  $d$  for jet injection angle  $\theta_o$ :  $45^\circ$ ,  $90^\circ$ ,  $135^\circ$  and  $Re_{cf}$ : 58202 & 104403

The radius of curvature increases with height in a uniform field because the fractional increase in the horizontal component of momentum flux decreases as more of the cross flow's momentum is taken into the jet [38]. The velocity ratio,  $R$  of the jet to the cross flow strongly affects the penetration depth of the jet and the mixing of two flow streams.

#### 4.4 Mixer pressure drop

Comparison of experimental results of pressure drop of all the cases is a vital part of determination of performance characteristics of the mixer examined. The pressure drop caused by a mixer flow configuration and jet injection can be expressed by a dimensionless ratio, Z-factor and also by pressure drop normalised with maximum pressure drop in the mixer during a set of runs for a particular injection angle. The Z factor is the ratio of pressure drop across the venturi-jet mixer ( $\Delta p_{VM}$ ) divided by the pressure drop in the empty pipe ( $\Delta p_{EP}$ ), which indicates an increase in energy costs when a static mixer is installed in a continuous flow process [39]. Therefore Z-factor can be written as given in Eq. (9):

$$Z = \frac{\Delta p_{VM}}{\Delta p_{EP}} \quad (9)$$

The Z-factor is examined in Fig. 9a as a function of the cross flow Reynolds number, indicating that it increases slowly for  $45^\circ$  injection angle. In contrast, for other injection angles up to a cross flow Reynolds of about 82000, the Z-factor drops sharply and beyond which it remains virtually constant at about 10. Many researchers report that Z-factors for the static mixers can range from 5 to 40, and our experimental results are within the specified range [40, 41]. Figure 9b represents the experimental pressure drop,  $\Delta p$  normalised with maximum pressure drop,  $\Delta p_{max}$  in the same set of

It is evident from the Fig. 8 that the jet penetrates deeper with increase in jet injection angle for the same cross flow Reynolds number. At sufficiently high cross flow speeds or low mass entrainment rates, a jet cannot only ingest significant quantities of motive fluid, but also the centreline of the jet can become distorted or bent-over in the cross flow field. The jet bends over because of the addition of horizontal momentum by the cross flow. A typical bent-over jet does not have a constant radius of curvature along its entire path.

experiments in the mixer. The experimental results for the pressure drop across the mixer for all the initial injection angles,  $\theta_0$  are compared for the studied venturi-jet mixer systems and plotted against cross flow Reynolds number,  $Re_{cf}$ . Figure 9b and 9c reveals that the maximum pressure drop occurs at higher value of cross flow Reynolds number due to the increase in inertial effects for all the cases of initial injection angles. For a particular injection angle, the pressure drop increases as the cross flow Reynolds number increases due to the appearance of counter rotating vortex pair at the diffuser outlet. The experimental result also reveals that the higher the value of cross flow Reynolds number  $Re_{cf}$  and initial injection angle  $\theta_0$  except  $60^\circ$ , the higher the pressure drop across the mixer. Thus, the initial injection angle and cross flow Reynolds number appear to have a significant effect on the mixer pressure drop. The pressure drop in the mixer is about 20% greater than the pressure drop in the venturi mixer without jet is observed from the experimental results of the present work.

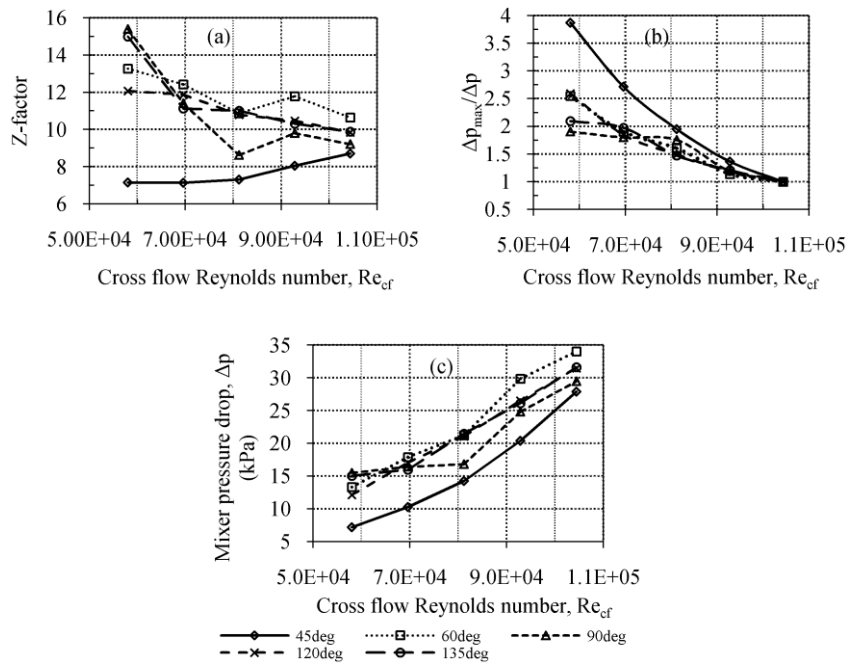


**Fig. 9** (a) Variation of Z-factor, (b) Normalised experimental pressure drop across the mixer (c) Mixer pressure drop Vs cross flow Reynolds number for inlet injection angles,  $45^\circ \leq \theta_0 \leq 135^\circ$

#### 4.5 Mixing index

To characterise the mixing performance by considering effects of arbitrary injection angle and increasing inertia on flow and mixing of venturi-jet mixer, the mixing index can be used to quantitatively [42 ,43]. The mixing efficiency,  $m_{eff}$  can be calculated by Eq. (10) as proposed by Jeon *et al.* [36].

$$m_{eff} = \left[ 1 - \frac{\int_0^W |c - c_{avg}| dx}{\int_0^W |c_o - c_{avg}| dx} \right] \times 100\% \quad (10)$$

where  $c_{avg}$  is the concentration of a complete mixing.

The pressure drop is a crucial factor to the design of a venturi-jet mixer device; therefore, the overall performance of venturi-jet mixer should include the evaluation of pressure drop. This overall

mixing performance is termed mixing index,  $m_{idx}$ , and used to evaluate the overall performance of a mixer. The mixing index is defined in Eq. (11).

$$m_{idx} = m_{eff} \times \frac{\Delta p_{max}}{\Delta p} \quad (11)$$

The experimental results of mixing index of the venturi-jet mixer are presented in Fig. 10 for all the cases of the present work. It is apparent that only a minor difference in the mixing index exists between the tested cross flows Reynolds number for a given injection angle. The results (Fig. 10) show that mixing index is greatest for the initial injection angle,  $\theta_o=120^\circ$  and lowest for the case of  $60^\circ$  injection. The increased mixing can be interpreted as the high injection angle causing the penetration of jet deeper into the cross flow and given more time for diffusion at the interface of the two liquids. However, the improvement of mixing performance is not proportional to the increased pressure drop. The criterion for designing a passive mixer should comprise the capability of a pump to overcome pressure drop with an adequate mixing efficiency. Therefore, the mixing efficiency has to compromise the pressure drop to optimize the design of a mixer [40]. The mixer with injection angle  $\theta_o \geq 90^\circ$  has approximately the same pressure drop, and more mixing. These results show that the optimized mixer would be one with injection angle  $\theta_o \geq 90^\circ$ .

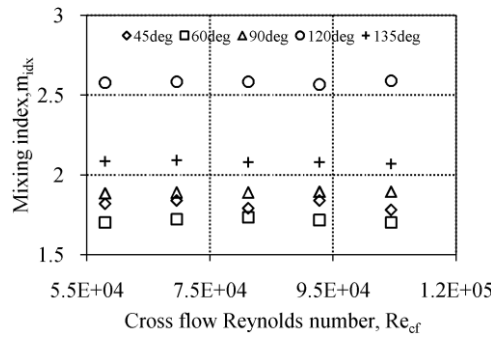


**Fig. 10** Mixing index,  $m_{idx}$  versus cross flow Reynolds number,  $Re_{cf}$

## 5. Conclusion

The trajectory of jet and mixing performance of the venturi-jet mixer has been investigated numerically through natural coordinate system of conservation equations and experimentally using concentration dilution and pressure drop measurements. For the present study, the results of numerical and experimental work are concluded as:

- The centreline concentration decay is rapid up to  $x=15d$  for  $\theta_o \leq 90^\circ$  and  $x=20d$  for  $\theta_o > 90^\circ$  because of quick expansion of jet due to turbulent entrainment.
- The jet centreline velocity increase at rapid rate upto  $s=5d$  and remains uniform thereafter for all the cases studied.
- The deeper the jet penetration into the cross flow for larger value of cross flow Reynolds number improves the mixing efficiency at the expense of faster increase of pressure drop.

- Improved mixer performance can be achieved with lower pressure drop for initial injection angle  $\theta_o \geq 90^\circ$ .
- The jet trajectory correlation obtained from the present work shows that jet penetration varies as the square root of downstream distance and one third root of velocity ratio. Also the effect of Reynolds number was included to study the jet penetration.

## Nomenclature

### Symbols

- $b$  - characteristic jet radius, [m]  
 $c$  - tracer concentration, [-]  
 $c_{avg}$  - concentration of a complete mixing, [-]  
 $d$  - diameter of jet, [m]  
 $D$  - throat diameter of venturi-jet mixer, [m]  
 $m$  - mass flow rate of fluid [ $\text{kg s}^{-1}$ ]  
 $m_{eff}$  - mixing efficiency, [-]  
 $m_{idx}$  - mixing index, [-]  
 $R$  - jet-to-mainstream velocity ratio, [-]  
 $Re$  - Reynolds number ( $=UD/\nu$ ), [-]  
 $s$  - axial jet arc length, [m]  
 $x$  - axial distance of venturi-jet mixer, [m]  
 $z$  - radial direction co-ordinate of venturi-jet mixer, [m]  
 $u$  - average (top-hat) jet velocity, [ $\text{ms}^{-1}$ ]  
 $u_e$  - local entrainment velocity, [ $\text{ms}^{-1}$ ]  
 $v$  - horizontal cross flow speed, [ $\text{ms}^{-1}$ ]  
 $\Delta p$  - overall pressure drop in the mixer, [kPa]  
 $\Delta p_{max}$  - maximum pressure drop across the mixer, [kPa]

### Subscripts

- $cf$  cross flow  
 $EP$  empty pipe  
 $j$  jet  
 $o$  initial condition  
 $VM$  venturi-jet mixer

### Greek letters

- $\alpha$  tangential entrainment parameter, [-]  
 $\beta$  normal entrainment parameter, [-]  
 $\gamma$  kinematic viscosity of fluid, [ $\text{ms}^{-2}$ ]  
 $\rho$  density of fluid, [ $\text{kg m}^{-3}$ ]  
 $\theta$  angle between jet axis and venturi-jet mixer centreline (deg)

## References

- [1] Hartung, H.K., Hiby, J.W., Acceleration of Turbulent Mixing in Tubes, *Chemical Engineering Journal*, 18 (1972), pp. 1051-1056.
- [2] Tauscher, W.A., Streiff, F.A., Static mixing of gases, *Chemical Engineering Progress*, 4 (1979), pp. 61-65.
- [3] Bain, D.B., Smith, C.E., Holdeman, J.D., CFD Assessment of Orifice Aspect Ratio and Mass Flow Ratio on Jet Mixing in Rectangular Ducts, AIAA 94-0218, (also NASA TM 106434), 1994.
- [4] Doerr, T.H., Blomeyer, M., Hennecke, D.K., Optimization of Multiple Jets Mixing with a Confined Cross flow, ASME Paper 95-GT-313, International Gas Turbine and Aeroengine Congress & Exposition, Houston, 1995.
- [5] Ho, C.M, Gummrk, E., Vortex Induction and Mass Entrainment in a Small-Aspect-Ratio Elliptic Jet, *Journal of Fluid Mechanics*, 179 (1987), pp. 383-405.
- [6] Gutmark, E., Schadow, K.C., Flow Characteristics of Orifice and Tapered Jets, *Physics of Fluids*, 30 (1987), 11, pp. 3448-3454.
- [7] Quinn, W.R., On Mixing in an Elliptic Turbulent Free Jet, *Physics of Fluids, A 1* (1989), 10, pp.1716-1722
- [8] Paterson, R.W., Turbofan Mixer Nozzle Flow Field: A Benchmark Experimental Study, *Journal of Engineering Gas Turbines and Power*, 106 (1984), pp. 692-698.
- [9] Eckerle, W.A., Sheibani, H., Awad, I., Experimental Measurement of the Vortex Development Downstream of a Lobed Forced Mixer, *Journal of Engineering Gas Turbines and Power*, 114 (1992), pp. 63-71.
- [10] Hu, H., Kobayashi, T., Saga, T., Taniguchi, N., Segawa, S., Ono, A., Research on the Mixing Enhancement Performance of Lobed Nozzle by using PIV and LIF, *Proceedings of 1998 ASME Fluids Engineering Division Summer Meeting*, FEDSM98-4994, 1998.
- [11] Ralph D.Collins, Beverly Hills, Don C. Willis, *US PATENT 3504702*, 1970.
- [12] Liscinsky, D.S., True, B., Effects of Inlet Flow Conditions on Cross-Flow Jet Mixing, *32nd Joint Propulsion Conference cosponsored by AIAA, ASME, SAE, and ASEE*, Florida, 1996.
- [13] Jean-Michel, Device for Mixing a Liquid Fertilizer with a Flow of Water for Use by Individuals, *US PATENT US 6,974,245 B2*, 2005.
- [14] Margason, R. J., Fifty Years of Jet in Cross flow Research, *In AGARD Symposium on a Jet in Cross Flow*, Winchester, UK, AGARD CP-534, 1993.
- [15] Maruyama, T., Mizushina, T., Watanabe, F., Turbulent Mixing of Two Fluid Streams at an Oblique Branch, *International Journal of Chemical Engineering*, 22 (1982), 2, pp. 287-294.
- [16] Maruyama, T., Suzuki, S., Mizushina, T., Pipeline Mixing between Two Fluid Streams Meeting at a T-Junction, *International Journal of Chemical Engineering*, 21 (1981), 2 pp. 205-212.
- [17] Adams, E.E., Dilution Analysis for Unidirectional Diffusers, *Journal of the Hydraulics Division*, ASCE, 108 (1982), 3, pp. 327-342.
- [18] Jirka, G.H., Multiport Diffusers for Heated Disposal: A Summary, *Journal of Hydraulics Division*, ASCE, 108 (1982), 12, pp. 1425-1443.
- [19] Chao, Y.C., Ho, W.C., Numerical Investigations of Heated and Unheated Lateral Jets Discharging into a Confined Swirling Cross flow, *Numerical Heat Transfer, Part A*, 22 (1992), pp. 343-361.

- [20] Sarkar, S., Bose, T. K., Comparison of Different Turbulence Models for Prediction of Slot-Film Cooling: Flow and Temperature Field, *Journal of Numerical Heat Transfer, Part B*, 28 (1995), pp. 217-238.
- [21] Su, L.K., Mungal, M.G., Simultaneous Measurements of Velocity and Scalar Fields: Application in Cross flowing Jets and Lifted Jet Diffusion Flames, *Center for Turbulence Research, Annual Research Briefs*, (1999), pp. 19-36.
- [22] Amighi, A., Eslamian, M., Ashgriz, N., Trajectory of a liquid jet in high pressure and high temperature subsonic air cross flow, *Proceedings of ICLASS*, (2009).
- [23] Stephen G. Monismith, Jeffrey R. Koseff, Janet K. Thompson, Catherine A. O’Riordan, Heidi M. Nepf, A Study of Model Bivalve Siphonal Currents”, *Limnol. Oceanogr.*, 35 (1990), 3, pp. 688-696.
- [24] Vyas, B. D., Kar, S., Standardisation of Water Jet Pumps, *Proceedings of Symposium on Jet Pumps and Ejectors*, Paper 10, BHRA Fluid Engineering, Cranfield, UK, 1972, pp. 155–170.
- [25] Raynerd, P., Ejectors, Selection and Use of Vacuum Equipment, *Institute of Chemical Engineering*, North Western Branch Papers, London, 1987, No. 1, pp. 3.1-3.16.
- [26] Bonnington, S.T., A Guide to Jet Pump Design, *British Chemical Engineering*, 3 (1964), pp. 150-154.
- [27] Sundararaj, S., Selladurai, V., Numerical and Experimental Study on Jet Trajectories and Mixing Behaviour of Venturi-Jet Mixer, *Journal of Fluids Engineering*, 132 (2010), 10, pp. 101104(1-9).
- [28] Li, Z., Murugappan, S., Gutmark, E., Vallet, L., Numerical simulation and experiments of jet in cross flow, 44<sup>th</sup> AIAA Aerospace Sciences Meeting and Exhibit, Reno, Nevada, AIAA 2006, 307.
- [29] Yuan, L.L., Street, R.L., Trajectory and Entrainment of a Round Jet in Cross Flow, *Journal of Physics of Fluids*, 10 (1998), pp.2323-2335.
- [30] Baylar, A., Ozkan, F., Ozturk, M., Influence of Venturi Cone Angles on Jet Aeration Systems, *Proceedings of International Civil Engineering and Water Management*, 158 (WMI), 2005, pp. 9-16.
- [31] Broadwell, J.E., Breidenthal, R.E., Structure and Mixing of a Transverse Jet in Incompressible Flow, *Journal of Fluid Mechanics*, 148 (1984), pp. 405-412.
- [32] Hault, D.P., Fay, J.A., Forney, L.J., A Theory of Plume Rise Compared with Field Observations, *Journal of Air Pollution Control Association*, 19 (1969), pp. 585-590.
- [33] Forney, L.J., Feng, Z., Wang, X., Jet Trajectories of Transverse Mixers at Arbitrary Angle in Turbulent Tube Flow, *International Transactions of Chemical Engineering*, 77 (1999), pp. 754-758.
- [34] Cozewith, C., Busko, M., Design Correlation for Mixing Tees, *Industrial and Chemical Engineering Research*, 28 (1989), 1521.
- [35] Kamotani, Y., Greber, I., Experiments on a Turbulent Jet in a Cross Flow. *AIAA Journal*, 10 (1992), 1425.
- [36] Leong, M.Y., McDonell, V.G., Samuelsen, G.S., Mixing of an Airblast-Atomized Fuel Spray Injected into a Cross Flow of Air, NASA Report No. NASA/CR-2000-210467.
- [37] Steven C. Chapra, Raymond P. Canale, Numerical Methods for Engineers, Tata McGraw Hill Publications, New Delhi, India, 2000.
- [38] Bursik, M., Effect of Wind on the Rise Height of Volcanic Plumes, *Geological Research Letters*, 28 (2001), 18, pp. 3621-3624.
- [39] Zalc, J.M., Szalai, E.S., Muzzio, F.J., Characterisation of Flow and Mixing in an SMX Static Mixer, *AIChE Journal*, 48 (2002), 3, pp. 427-436.

- [40] Paul, M.H., Muschelknautz, E., Static Mixers and their Applications, *International Journal of Chemical Engineering*, 22 (1982), 197.
- [41] Alloca, P.T., Mixing Efficiency of Static Mixing Units in Laminar Flow, *Fibre Producer*, 12 (1982).
- [42] Wang, H., Iovenitti, P., Harvey, E., Masood, S., Mixing of Liquids using Obstacles in Microchannels, *Proceedings of SPIE, BioMEMS and Smart Nanostructures*, Adelaide, Australia, 2001, 4590, pp. 204-212.
- [43] Jeon, N. L., Dertinger, S. K.W., Chiu, D. T., Choi, I. S., Stroock, A. D., Whitesides, G. M., Generation of Solution and Surface Gradients using Microfluidic Systems, *Langmuir*, 16 (2000) 22, pp. 8311–8316.

Authors' Affiliations:

S. *SUNDARARAJ* (**corresponding author**)

Department of Mechanical Engineering,  
Sri Krishna College of Engineering and Technology,  
Kuniamuthur Post, Coimbatore 641 008  
Tamilnadu, India.

**E-mail:** [papers.sundar@yahoo.co.in](mailto:papers.sundar@yahoo.co.in)

*Dr. V.SELLADURAI*

Department of Mechanical Engineering,  
Coimbatore Institute of Technology,  
Coimbatore, Tamilnadu, India.